JOURNAL OF NATURAL PRODUCTS

Article

pubs.acs.org/jnp

Xanthohumol Induces Apoptosis in Human Malignant Glioblastoma Cells by Increasing Reactive Oxygen Species and Activating MAPK Pathways

Michela Festa,[†] Anna Capasso,*[,†] Cosimo W. D'Acunto,[†] Milena Masullo,[†] Adriano G. Rossi,[‡] Cosimo Pizza,[†] and Sonia Piacente*[,†]

[†]Dipartimento di Scienze Farmaceutiche e Biomediche, Università degli Studi di Salerno, Via Ponte Don Melillo, 84084 Fisciano, Salerno, Italy

[‡]MRC Centre for Inflammation Research, The Queen's Medical Research Institute, University of Edinburgh Medical School, EH16 4TJ, Edinburgh, U.K.

S *Supporting Information*

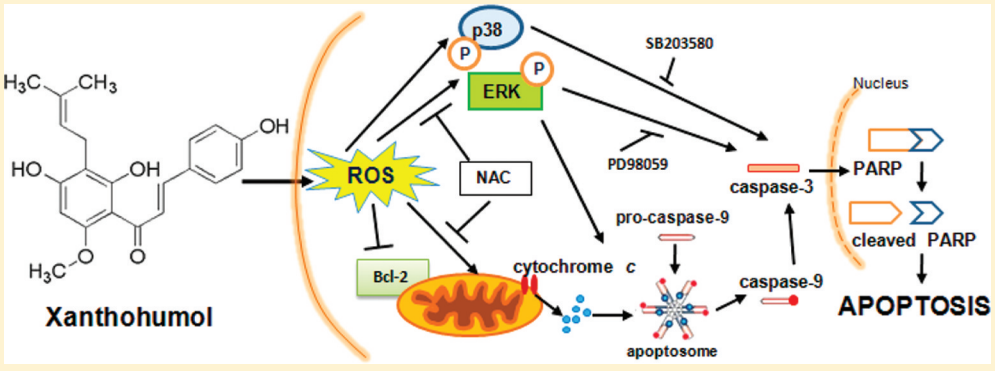

ABSTRACT: The effect of the biologically active prenylated chalcone and potential anticancer agent xanthohumol (**1**) has been investigated on apoptosis of the T98G human malignant glioblastoma cell line. Compound **1** decreased the viability of T98G cells by induction of apoptosis in a time- and concentration-dependent manner. Apoptosis induced by **1** was associated with activation of caspase-3, caspase-9, and PARP cleavage and was mediated by the mitochondrial pathway, as exemplified by mitochondrial depolarization, cytochrome *c* release, and downregulation of the antiapoptotic Bcl-2 protein. Xanthohumol induced intracellular reactive oxygen species (ROS), an effect that was reduced by pretreatment with the antioxidant *N*-acetyl-L-cysteine (NAC). Intracellular ROS production appeared essential for the activation of the mitochondrial pathway and induction of apoptosis after exposure to **1**. Oxidative stress due to treatment with **1** was associated with MAPK activation, as determined by ERK1/2 and p38 phosphorylation. Phosphorylation of ERK1/2 and p38 was attenuated using NAC to inhibit ROS production. After treatment with **1**, ROS provided a specific environment that resulted in MAPK-induced cell death, with this effect reduced by the ERK1/2 specific inhibitor PD98059 and partially inhibited by the p38 inhibitor SB203580. These findings suggest that xanthohumol (**1**) is a potential chemotherapeutic agent for the treatment of glioblastoma multiforme.

Glioblastoma multiforme (GBM) (WHO grade IV) is the most common tumor of the central nervous system (CNS) in humans and is particularly highly aggressive and invasive, exhibiting rapid cell growth, resistance to apoptosis, and robust angiogenesis. Unfortunately, the median survival of GMB patients is 6−12 months from the time of diagnosis, and current treatments, including surgery, radiation therapy, and chemotherapy have not significantly improved the prognosis.[1] The major limitations of chemotherapy for the treatment of GBM are the inability of many drugs to pass through the blood−brain barrier and their low efficacy in inducing apoptosis. Therefore, the choice of effective drugs is limited, and new therapeutic strategies are needed urgently. There is increasing evidence that several natural compounds found in plants may be useful as cancer chemotherapeutic or chemopreventive agents. Moreover, there is strong evidence showing that structurally different flavonoids are able to traverse the blood−brain barrier in vivo.[2] Xanthohumol (**1**) is one of the major prenylated phenolic constituents occurring in the hop cones of *Humulus lupulus* L. (Cannabaceae). Hops are used traditionally to add bitterness and flavor to beer; however, more recently, alternative uses for hop polyphenols and their effect on several biological processes have become apparent. Limited in vitro studies indicate that several prenylated polyphenolic constituents occurring in the hop plant possess possible

Received: May 6, 2011
Published: November 23, 2011

dx.doi.org/10.1021/np200390x | *J. Nat. Prod.* 2011, 74, 2505−2513

anticarcinogenic properties. In particular, xanthohumol (**1**) has received major attention because it has been shown to inhibit the initiation, promotion, and progression stages of carcinogenesis, hence behaving as a potential broad-spectrum chemopreventive agent.[3] The cytotoxic activities of several beer polyphenols, including **1**, have been investigated in various cell lines. For example, this compound inhibits human breast (MCF-7), colon (HT-29), ovarian (A2780), and prostate (DU145, PC-3) cancer[4] and B-chronic lymphocytic leukemia cell proliferation[5] and induces apoptosis in human breast and prostate cancer cells in vitro.[6] In addition, pro-apoptotic effects of a hop-bitter acid, humulone (**2**), in the leukemia cell lines HL60 and U937 have also been reported.[7]

A recent in vivo study showed the ability of xanthohumol (**1**) to induce a significant inhibition of angiogenesis in mice implanted with a Matrigel sponge when administered in drinking water at a concentration of 2 μM. At a higher concentration of 200 μM, **1** displayed marked angiogenesis inhibition without adverse effects on animal health parameters.[8] It has also been shown that **1** targets tumor growth and angiogenesis in Kaposi's sarcoma tumor in male nude mice.[9]

Phenolics are generally considered to be antioxidants, but most of them behave as powerful pro-oxidant molecules.[10] Compound **1** has been reported to exert antioxidant activity,[11] but very recently it also appeared to induce transient superoxide anion radical formation triggering cancer cell apoptosis.[12] Reactive oxygen species (ROS), such as superoxide anion ($O_2\cdot^-$), hydrogen peroxide (H_2O_2), and hydroxyl radical (HO·), influence many biological processes, including apoptosis.[13] The redox state of the cells is a crucial factor in deciding its susceptibility to apoptotic stimuli. ROS at low concentrations act as intracellular messengers regulating several processes including cell proliferation, while the production of large amounts of ROS promotes apoptosis.[14]

Some flavonoids are reported to trigger apoptosis through modulation of different signal transduction pathways, such as the phosphatidyinositol-3-kinase/Akt and mitogen-activated protein kinase (MAPK) pathways, which may affect cellular function by modulating gene regulation or phosphorylating proteins.[15] Furthermore, they can directly or indirectly affect the activity and expression of key proteins (e.g., caspases and Bcl-2 family members) involved in the regulation of apoptosis. Moreover, it has been reported that certain flavonoids induce apoptosis in human glioblastoma T98G and U87MG cells, but not in human normal astrocytes through the increase of ROS production, changes in mitochondrial membrane potential ($\Delta\Psi$m), and phosphorylation of MAPKs.[16] More recently, xanthohumol (**1**) has been shown to be an attractive candidate for the regulation of inflammatory responses in the brain, showing anti-inflammatory activity in microglial BV2 cells.[17] Since the effects of beer polyphenols have never been investigated in brain cancer and, in particular, in malignant glioblastoma, we have studied the molecular mechanism by which **1** induces apoptosis in human glioblastoma cells. We report herein that the pro-apoptotic effect of **1** in human glioblastoma cells is mediated by increasing ROS production, and activation of the MAPK (ERK1/2) phosphorylation cascade and involves the mitochondrial pathways. This study therefore provides evidence, for the first time, that xanthohumol can be considered as a potential chemotherapeutic agent for the treatment of glioblastoma multiforme.

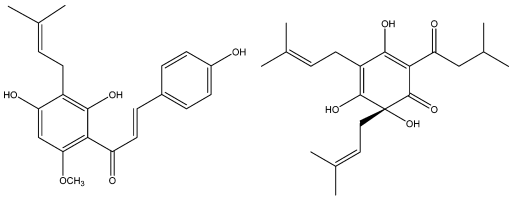

xanthohumol (**1**) humulone (**2**)

RESULTS AND DISCUSSION

Xanthohumol (1) Decreases Cell Viability and Induces Apoptosis in Human Glioblastoma Cells. To examine the antitumor potential of the two polyphenols isolated from *H. lupulus*, xanthohumol (**1**) and humulone (**2**), on GBM, their effects were investigated on cell viability using two human glioblastoma cell lines (T98G, U87-MG) and a normal human astrocyte cell line (NHA) (Figure 1A). Cells were treated with different concentrations of **1** and **2** (1−50 μM) for 48 h, and then cell viability was assessed using the MTT assay. DMSO was used as a control (100% cell viability). Compound **1** strongly decreased cell viability in T98G cells in a concentration-dependent manner (significant effects were observed at 10 μM, and up to 70% loss of viability was noted with 50 μM **1**), whereas a small but significant effect was observed at the highest concentration tested (50 μM) on cell viability of U87-MG cells. Humulone treatment did not affect the viability of the two cancer cell lines, not even at a higher concentration of 50 μM (Figure 1A). Interestingly, both compounds **1** and **2** did not affect viability of NHA cells, pointing out a certain degree of selectivity against cancer cells (Figure 1A). The effects of **1** and **2** on cell cycle progression of glioblastoma cells using flow cytometry were also analyzed. Neither **1** nor **2** at the concentrations tested caused changes in the phases (G0/G1, G2/M, and S) of the cell cycle in T98G and U87-MG cells after 48 h treatment (Figure 1B). To ascertain whether loss of cell viability was mediated by apoptosis, the effects of **1** and **2** were analyzed on apoptosis of T98G and U87-MG cells using propidium iodide staining of DNA fragmentation after cell permeabilization. Cells were treated with different concentrations of **1** and **2** (1−50 μM) for 24 and 48 h, and then the population of sub-G1 cells (hyplodiploid nuclei) was determined. Xanthohumol induced apoptosis of T98G cells in a concentration-dependent manner with 40% cell death at 20 μM after 48 h, whereas a small pro-apoptotic effect was observed at 50 μM in U87-MG cells. Apoptosis was not triggered by **2** in both the glioblastoma cell lines (Figure 1C). These results revealed that T98G cells were more sensitive than U87-MG cells to the action of xanthohumol and that this compound causes death in T98G cells by induction of an apoptotic mechanism. Thus, in order to further dissect the underlying mechanisms involved in the pro-apoptotic effects of **1**, T98G cells were used.

Xanthohumol (1) Induces Apoptosis by Caspase Activation and PARP Cleavage. Caspases play a central role in mediating most apoptotic responses. To analyze the apoptotic pathway and the role of caspases involved in apoptosis of T98G cells mediated by **1**, apoptosis was examined in the presence of the pan-caspase inhibitor Z-VAD-FMK. Pretreatment of cells with Z-VAD-FMK (25 μM) strongly inhibited the percentage of apoptotic cells after treatment with **1**, suggesting that apoptosis is associated with caspase activation (Figure 2A). Western blot analysis of the expression levels of caspase-3 and caspase-9 after exposure to **1** for different times

(Figure 2B) showed the involvement of these effector caspases. Xanthohumol induced caspase-3 activation after 24 h, whereas the upstream caspase-9 was activated only after 8 h of incubation by this compound, indicating that the death signaling is mediated through the mitochondrial pathway. Expression of poly(ADP-ribose) polymerase (PARP), a protein targeted and cleaved by caspases during apoptosis, was also examined. Xanthohumol inactivated PARP, as indicated by the appearance of the 89 kDa fragment after 24 h of treatment.

Xanthohumol (1) Induces Apoptosis through the Mitochondrial Pathway. Mitochondrial changes, including permeability transition pore opening and the collapse of AΨm, result in the release of cytochrome *c* into the cytosol, which subsequently causes apoptosis by the activation of caspases.[18] Figure 3A shows that treatment of T98G cells with **1** resulted in a time-dependent increase of the number of cells with depolarized mitochondria as early as 4 h, with sustained effects

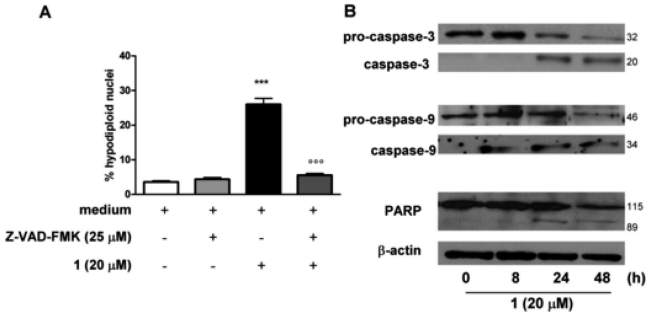

Figure 2. (A) Effects of the caspase inhibitor Z-VAD-FMK (25 μM) pretreatment on xanthohumol (**1**)-induced apoptosis in T98G cells (means ± SEM of three experiments performed in triplicate; ***p < 0.001 vs control cells, °°°p < 0.001 vs **1** in the presence of Z-VAD-FMK). (B) Western blotting analysis of caspase-3, caspase-9, and PARP protein expression after incubation with **1** (20 μM) at different times. Blots are representative of three different experiments.

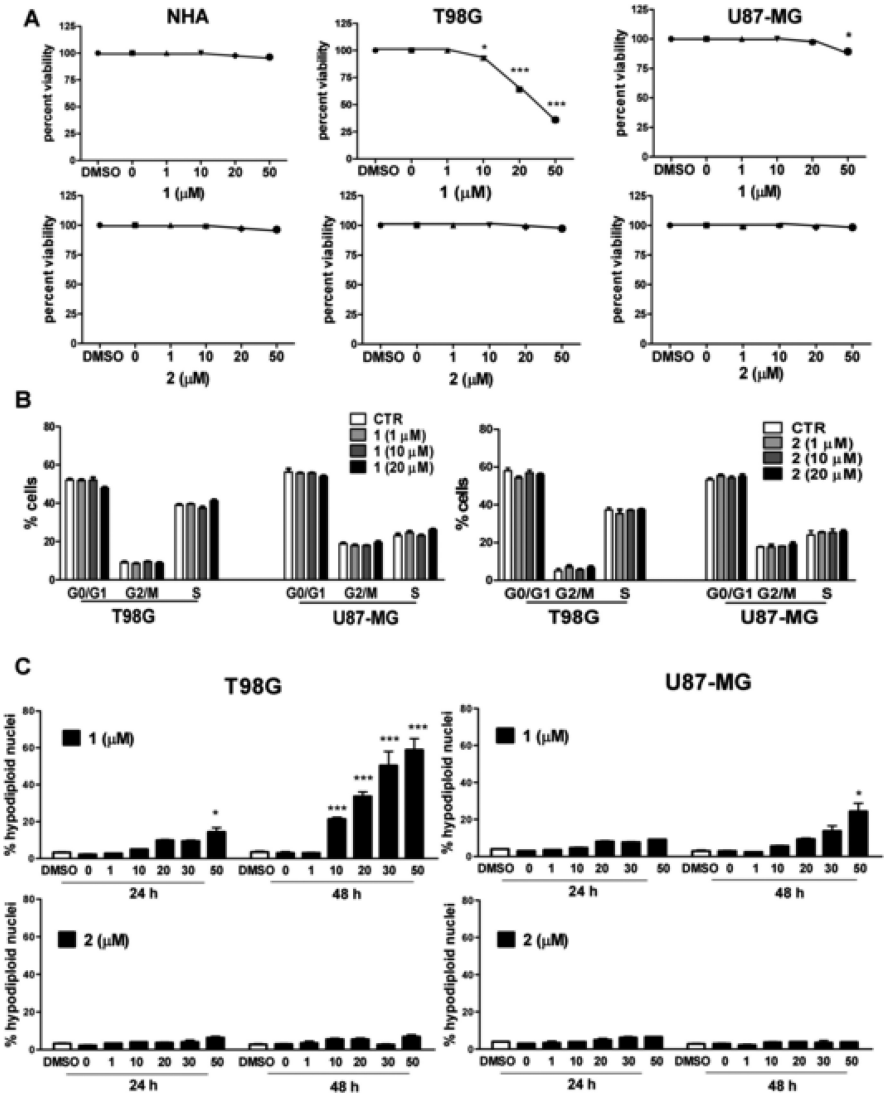

Figure 1. Effects of xanthohumol (**1**) and humulone (**2**) on cell viability (A), cell cycle progression (B), and apoptosis (C) of human glioblastoma cells (T98G, U87-MG) and normal astrocytes (NHA). Cell viability was assayed using the MTT assay after incubation with different concentrations (1−50 μM) of **1** and **2** and DMSO (0.1%) alone for 48 h (*p < 0.05, ***p < 0.001 vs T98G control cells,*p < 0.05 vs U87-MG control cells). For cell cycle progression analysis, cells were treated with **1** and **2** (1−20 μM) for 48 h, and then the percentage of cells in the G1, S, and G2/M phases was calculated by flow cytometry analysis. The percent of apoptotic cells (hypodiploid) treated with different concentrations of **1** and **2** (1−50 μM) for 24−48 h was analyzed using flow cytometry propidium iodide staining. (*p < 0.05 vs U87-MG 48 h control cells; *p < 0.05 vs T98G 24 h control cells, ***p < 0.001 vs T98G 48 h control cells). Results are expressed as means ± SEM of three experiments performed in triplicate.

dx.doi.org/10.1021/np200390x | *J. Nat. Prod.* 2011, 74, 2505−2513

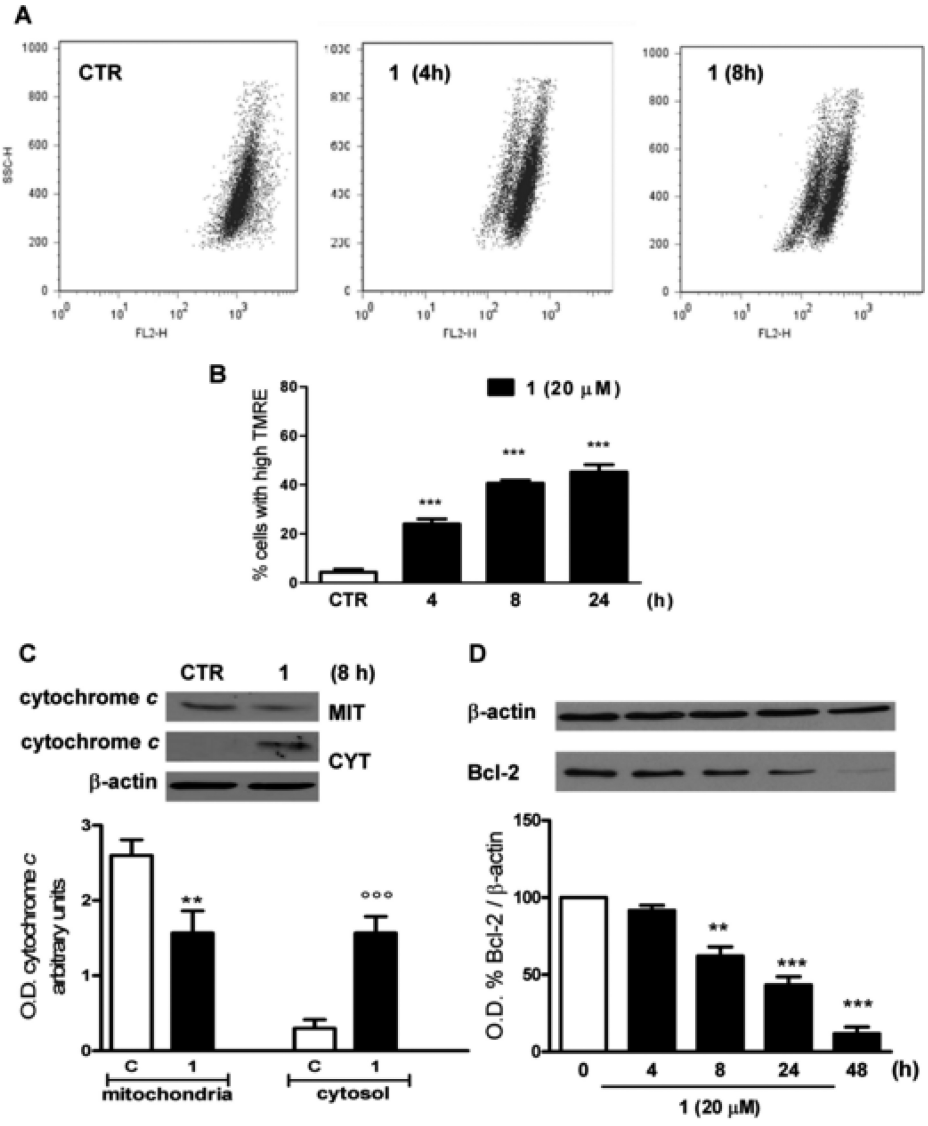

Figure 3. Effects of xanthohumol (**1**) on mitochondrial membrane depolarization, cytochrome *c* release, and Bcl-2 expression in T98G cells. (A) Representative flow cytometry profiles of control and cells treated with **1** (20 μM) following TMRE loading. (B) Percentage of T98G cells with high TMRE fluorescence (cells with depolarized mitochondria) treated with or without **1** (4−24 h) (***$p < 0.001$ vs untreated cells, results are expressed as means ± SEM of three experiments performed in triplicate). (C) Western blot analysis for cytochrome *c* release from cytosol to mitochondria in T98G cells treated with **1** for 8 h (**$p < 0.01$ vs mitochondria C, °°°$p < 0.001$ vs cytosol C). (D) Western blotting of Bcl-2 expression after treatment with **1** for different times (0−48 h). (**$p < 0.01$, ***$p < 0.001$ vs untreated cells). All blots are representative of three different experiments with similar results, and *β*-actin antibody was used to verify equal load of proteins analyzed.

observed at 24 h (50% cells with high TMRE fluorescence), as indicated in Figure 3B. Compound **1** was found also to cause a mitochondrial membrane permeability transition, as determined by Western blot analysis of the release of cythocrome *c* from the mitochondria into the cytosol in cells exposed to the drug for 8 h (Figure 3C). Moreover, **1** decreased expression of Bcl-2, an antiapoptotic protein associated with mitochondrial integrity, in a time-dependent manner with a maximum effect observed after 48 h (Figure 3D). These results suggest that the mitochondrial pathway is likely involved in the cell death mechanisms induced by **1** in T98G cells.

Xanthohumol (1) Triggers ROS Production in T98G Cells. Alterations of the intracellular redox balance are known to play a regulatory role in cell death. Xanthohumol has been reported to elevate intracellular ROS levels at early time points and to induce leukemic cell apoptosis.[19] When ROS production was measured after exposure of T98G cells to **1** at different times (5−120 min) by flow cytometric analysis of DCFH-DA fluorescence intensity (Figure 4A), it was observed that ROS intracellular levels were increased as early as 5 min after exposure. ROS production induced by **1** was attenuated effectively by pretreatment with the antioxidant *N*-acetyl-L-cysteine (NAC) at all the time points analyzed. These results were confirmed by observation of intracellular ROS production in the presence and absence of NAC using fluorescence microscopy (Figure 4B).

Xanthohumol (1)-Induced Apoptosis in T98G Cells Is Mediated by ROS Generation. The role of ROS in mediating apoptosis in various cancer cells is well established.[19] Therefore, it was investigated whether or not oxidative stress caused xanthohumol-induced apoptosis. It was observed that **1** generated intracellular ROS production at 24 h and that NAC abolished this effect observed by flow cytometry and fluorescence microscopy (Figure 5A). To determine whether

dx.doi.org/10.1021/np200390x | *J. Nat. Prod.* 2011, 74, 2505−2513

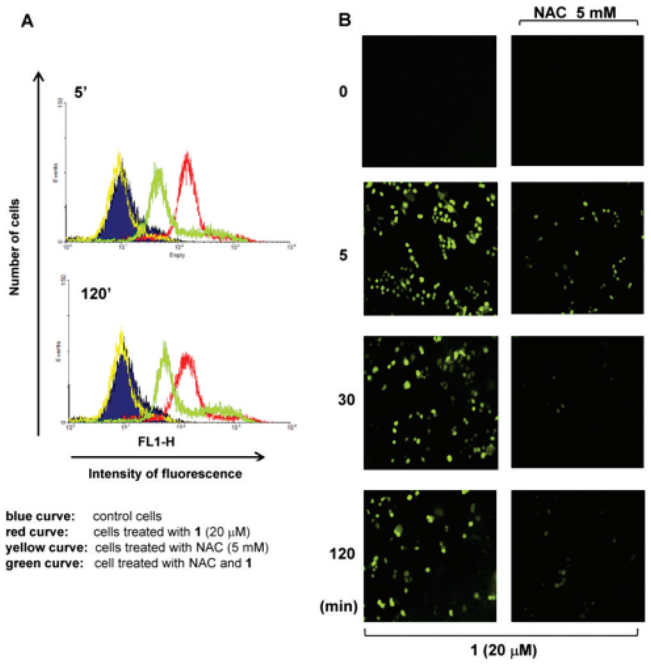

Figure 4. Effect of **1** on intracellular ROS generation at early time points in T98G cells. (A) Flow cytometry histograms of fluorescence (FL-1 channel) of DCFH-DA in cells treated with **1** (20 μM), with or without NAC (5 mM) pretreatment, for 5−120 min. (B) Production of intracellular ROS observed by fluorescence microscopy (magnification 40×) after treatment with **1** (5−120 min) with or without NAC pretreatment. Results are representative of three experiments performed in duplicate.

increased production of ROS was critical for **1**-induced apoptosis, cells were pretreated in the presence and absence of two different antioxidant agents, NAC (5 mM) and ascorbic acid (10 μM), and then analyzed for apoptosis after exposure of **1** for 48 h. The results in Figure 5B show that apoptosis induced by **1** was reduced significantly in the presence of either NAC or ascorbic acid. The mitochondrial depolarization and expression of Bcl-2 and PARP proteins were analyzed in the presence of NAC with or without treatment with 20 μM **1**. NAC pretreatment inhibited the percentage of depolarized cells after treatment with **1**, suggesting the involvement of ROS in the activation of the mitochondrial pathway (Figure 5C). Western blots shown in Figure 5D demonstrate that Bcl-2 downregulation and PARP cleavage induced by **1** were partially reversed and completely abolished, respectively, after pretreatment with NAC. These results indicated that **1** induced apoptosis by a mechanism requiring the increase of intracellular ROS levels in T98G cells.

ROS Induces MAPK Activation Leading to Apoptosis of T98G Cells. Generation of intracellular ROS is known to activate the MAPK pathway[20] with MAPKs being relevant in apoptosis signaling.[21] Since **1** enhanced the levels of intracellular ROS in T98G cells, the involvement of MAPK signaling by Western blotting analysis of phosphorylated ERK1/2 and p38 expression was examined after treatment with **1**. Phosphorylation of ERK1/2 strongly increased after 5 min and was sustained at 2 h following exposure to **1** (Figure 6A), whereas p38 phosphorylation was induced transiently at 30−60 min after treatment with this compound (Figure 6B). No activation of JNK/SAPK (c-Jun N-terminal kinase/stress-activated protein kinase) was observed after treatment with **1** (data not shown). To demonstrate that ROS production is involved in MAPK activation, the phosphorylation of ERK1/2 and p38 was evaluated in the presence of NAC with and without treatment with **1**. ERK1/2 and p38 phosphorylation induced by **1** decreased significantly with NAC pretreatment, indicating that ROS induced by this compound are upstream regulators of MAPK signaling (Figure 6B). Evidence suggests that the activation of ERK1/2 has a death-promoting role in different cell types regulating different signaling molecules of apoptotic machinery.[22] It was found also that **1** is able to induce a dramatic phosphorylation of ERK after 24 h and that this effect is partially abolished by NAC pretreatment (Figure 6C), suggesting an important role of ERK in the apoptotic signaling by **1**, whereas p-38 activation was not observed at late time points (data not shown). To confirm the importance of MAPK signaling in **1**-induced apoptosis, the levels of apoptosis were evaluated in the presence of specific MAPK inhibitors. Cells were pretreated with the ERK inhibitor PD98059 (20 μM) for 30 min, the p38 MAPK inhibitor SB203580 (5 μM) for 1 h, or the JNK inhibitor SP600125 (5 μM) for 1 h and then treated with 20 μM **1** for 48 h. Flow cytometric analysis of apoptosis showed that pretreatment with PD98059 reduced cell apoptosis significantly, by 50%, whereas a partial reduction was observed with the p38 inhibitor (Figure 6D). The JNK inhibitor did not influence **1**-induced apoptosis, suggesting that this kinase is not implicated in this mechanism. These results revealed that initially activation of ERK and then p38 is involved in **1**-induced apoptotic cell death.

Initially, the effects of the polyphenols xanthohumol (**1**) and humulone (**2**) were investigated on the viability of normal human astrocytes (NHA) and of two cancer cell lines, T98G and U87-MG, representing the highest stages of malignancy of glioblastoma in vitro models. Compound **1** strongly decreased viability of T98G cells at 20 μM, whereas a small effect was observed at the highest concentration tested (50 μM) in U87-MG cells. Interestingly, **1** showed activity against glioblastoma cells and no cytotoxicity in normal human astrocytes. Compound **1** was able to induce apoptosis in T98G cells in a concentration-dependent manner, while in U87-MG cells a minor apoptotic effect was observed only at the highest concentration used. In turn, compound **2** showed no effects in the analyzed cell lines. Hence, the mechanisms of **1**-induced apoptosis in the T98G cell line were determined at 20 μM concentration. Xanthohumol induced apoptosis by activating caspases-3 and -9 and inducing cleavage of PARP. Activation of caspase-9 indicated how the death signaling can be mediated through an intrinsic apoptotic pathway. Compound **1** induced mitochondrial depolarization by inhibiting Bcl-2 expression in a time-dependent manner and consequently leading to the release of cytochrome *c* in the cytosol. Bcl-2 protein can prevent ROS production and regulates the mitochondrial transitional pore opening, blocking cytochrome *c* release and inhibiting caspases. A variety of cellular functions, including proliferation, growth arrest, and cell death, are regulated by oxidative stimuli. Several natural polyphenols have been proposed to induce oxidative stress indirectly by targeting the mitochondrial electron transport chain, thereby generating a downstream flux of ROS.[23] Compound **1** strongly increased ROS intracellular production at early time points, with sustained effect after 24 h treatment. To determine whether the ROS production increase was critical to **1**-induced apoptosis, cells were pretreated with NAC and ascorbic acid, reducing the percentage of apoptosis. NAC inhibited

dx.doi.org/10.1021/np200390x | *J. Nat. Prod.* 2011, 74, 2505−2513

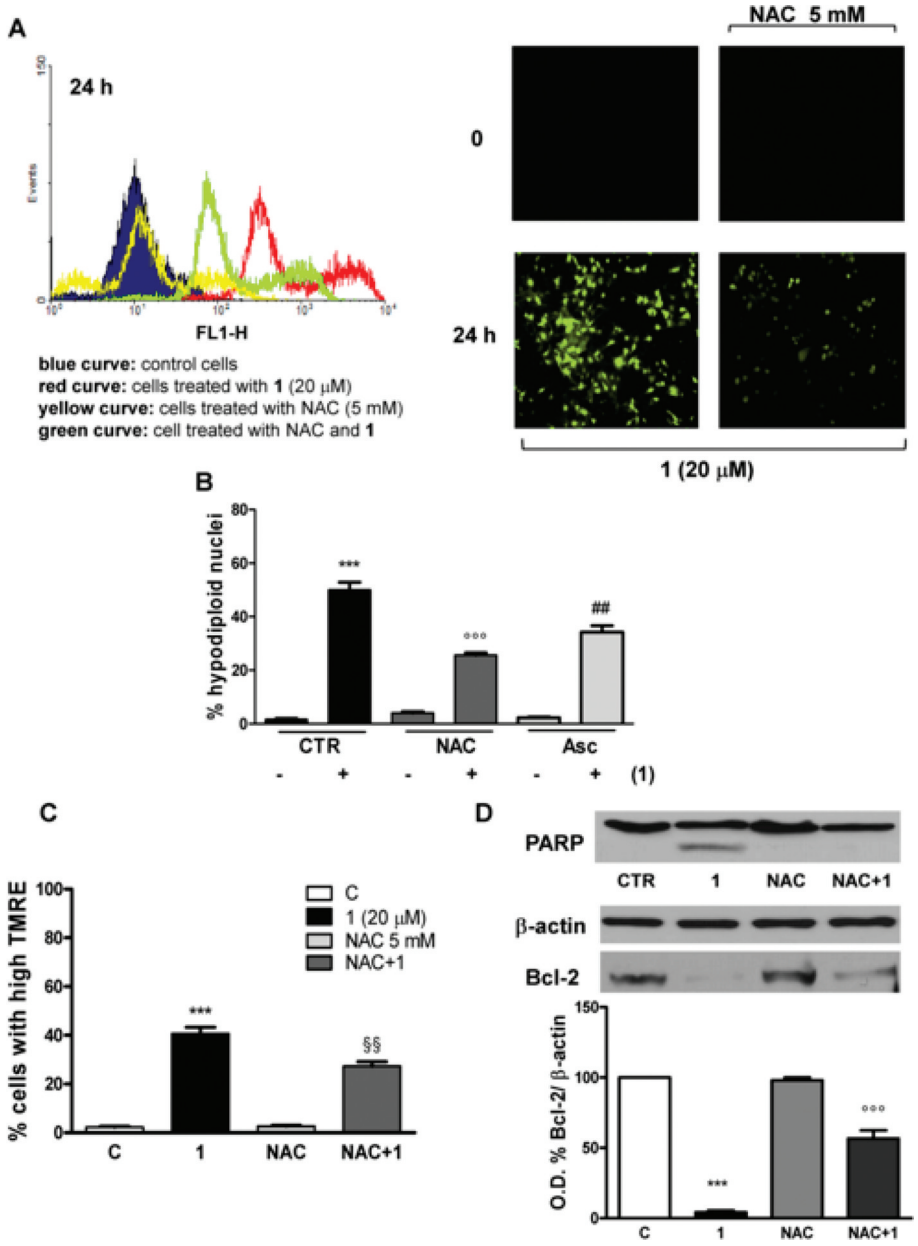

Figure 5. Involvement of ROS production on xanthohumol (**1**)-mediated apoptosis in T98G cells. (A) Intensity of fluorescence of DCFH-DA measured by flow cytometry and fluorescence microscopy (magnification 40×) after treatment with **1** (20 μM) for 24 h with or without NAC (5 mM). (B) Effects of NAC (5 mM) and ascorbic acid (10 μM) on xanthohumol-mediated apoptosis in T98G cells by propidium iodide flow cytometry analysis (n = 4, ***p < 0.001 vs control cells, $^{\#\#}p$ < 0.01, $^{\circ\circ\circ}p$ < 0.001 vs **1**-treated cells). (C) Effect of NAC on mitochondrial depolarization induced by **1**. The percentage of cells with depolarized mitochondria was evaluated by flow cytometry using TMRE loading (n = 3, ***p < 0.001 vs control cells, $^{\S\S}p$ < 0.01 vs **1**-treated cells). (D) Effect of NAC pretreatment on **1**-induced PARP cleavage and Bcl-2 downregulation by Western blot (***p < 0.001 vs control cells, $^{\circ\circ\circ}p$ < 0.001 vs **1**-treated cells). Blots are representative of three experiments with similar results.

mitochondrial depolarization and Bcl-2 downregulation induced by **1**. These results indicate how the increase of intracellular ROS is essential to induce apoptosis and to activate the mitochondrial pathway after exposure to **1** in T98G cells. A direct relationship between alteration of the intracellular redox state and the activation of MAPK pathways has been clearly demonstrated.[24] Moreover, a role for polyphenols in the activation of different MAPK members has been suggested as a necessary event for downstream induction of apoptosis in cancer cells.[25] Exposure of cells to oxidant stress also induces activation of multiple MAP kinase pathways.[26] Increasing evidence suggests that ERK activation contributes to apoptosis in certain cell types and organs under different conditions and stimuli.[27] Xanthohumol induced rapid ERK1/2 phosphorylation after 5 min, and it persisted after 24 h. Prolonged activation of ERK1/2 seems to lead to cell death.[28] Xanthohumol-induced apoptosis is mediated mainly by ERK activation and partially by p38, phophorylated by **1** transiently just at early time points. Moreover inhibition of ERK1/2 with the specific inhibitor PD98059 and of p38 with SB203580 reduced **1**-induced apoptosis. Phosphorylation of ERK1/2 and p38 induced by **1** was abrogated by NAC, suggesting how the increase of ROS produces a specific environment leading to MAPK-mediated cell death. Finally, the different responsiveness of glioblastoma

dx.doi.org/10.1021/np200390x | J. Nat. Prod. 2011, 74, 2505–2513

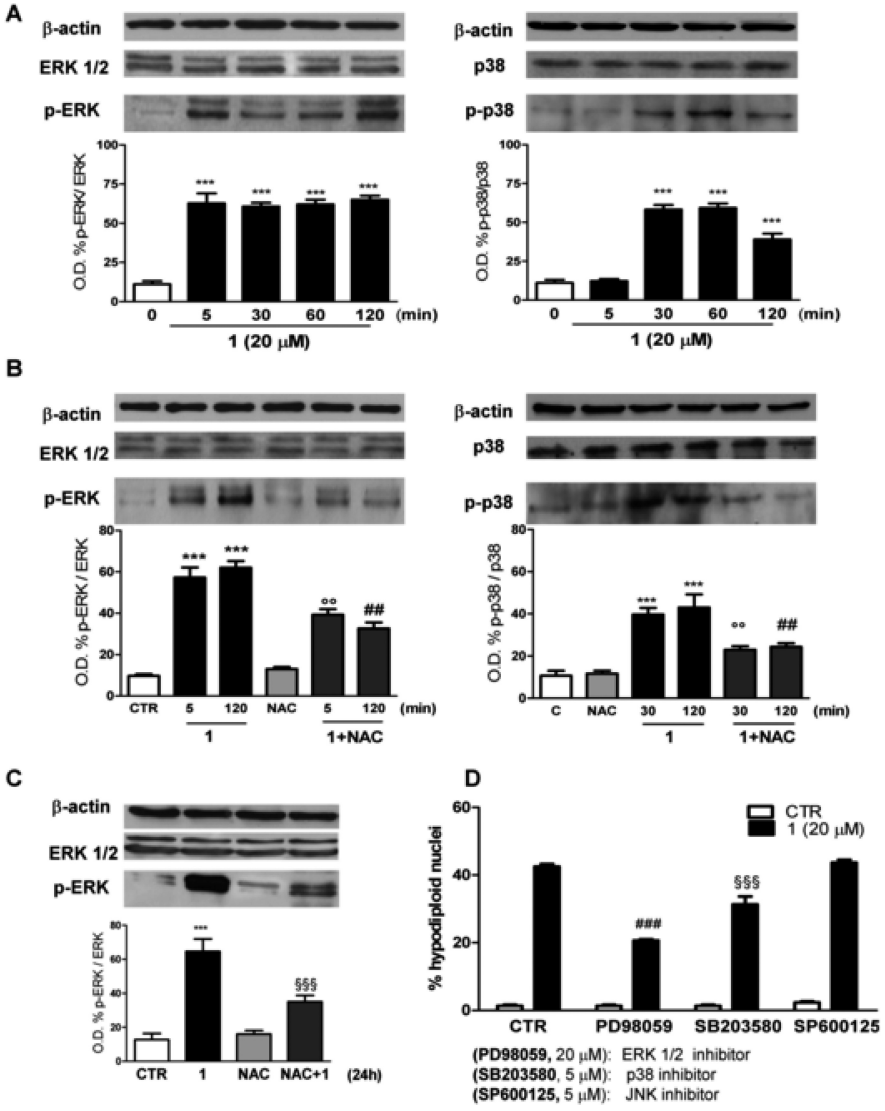

Figure 6. Involvement of MAPK pathway in **1**-induced and ROS-mediated apoptosis in T98G cells. (A) Western blotting of ERK1/2 and p38 phosphorylation after treatment with **1** (20 μM, 5−120 min). (B) Effect of NAC (5 mM) on phosphorylation of ERK1/2 and p38 analyzed by Western blot (***p < 0.001 vs C cells, °°p < 0.01 vs 5 and 30 min **1**-treated cells, ##p < 0.01 vs 120 min **1**-treated cells). (C) Western blotting analysis of ERK activation at 24 h with **1** and NAC treatments (***p < 0.001 vs C cells, §§§p < 0.001 vs **1**-treated cells). All blots are representative of three experiments with similar results, and total ERK1/2 and p38 were used to normalize p-ERK and p-p38 protein expression. (D) Effects of pretreatment with 20 μM ERK1/2 inhibitor (PD98059) for 30 min, 5 μM p-38 MAPK inhibitor (SB203580) for 1 h, and 5 μM JNK inhibitor (SP600125) for 1 h on **1**-induced apoptosis after 48 h analyzed by flow cytometry (###p < 0.001, §§§p < 0.001 vs **1**-treated control cells; results are expressed as means ± SEM of three experiments performed in triplicate).

cell lines to compound **1** might be due to the different status of p53 in T98G (mutated) and U87-MG (wild type) cells. The p53 tumor suppressor gene controls growth, DNA repair, cell cycle arrest, and apoptosis.[29] T98G cells were more sensitive to compound **1** probably because xanthohumol induced phosphorylation of p53 (Ser46), leading cells to apoptosis, whereas in U87-MG cells p53 phosphorylation was not observed (Figure S1, Supporting Information). Due to the potential beneficial biological activities of compound **1**, increasing attention has been focused on its application to humans as a medicine or dietary supplement. Previous toxicological studies in mice have demonstrated the safety of **1**, showing an LD_{50} for oral dose of hop extract ranging from 500 to 3500 mg/kg,[4] while oral administration of this compound to mice did not affect major organ functions or metabolism.[6] Thus, xanthohumol has potential as a chemotherapeutic agent in the treatment of GBM, inducing apoptosis in T98G cells by a complex mechanism (Figure S2, Supporting Information). Further work should be performed using in vivo models to better understand the potential application of **1** in the management of glioblastoma multiforme.

EXPERIMENTAL SECTION

General Experimental Procedures. NMR experiments were performed on a Bruker DRX-600 spectrometer (Bruker BioSpinGmBH, Rheinstetten, Germany) equipped with a Bruker 5 mm TCI CryoProbeat 300 K. All NMR spectra were acquired in CD_3OD (99.95%, SigmaAldrich) and processed using UXNMR software. ESIMS were performed using a ThermoFinnigan LCQ Deca ion trap mass spectrometer equipped with Xcalibur software. HPLC separations were carried out on an Agilent 1100 series chromatograph, equipped with a G-1312 binary pump, a G-1328A rheodyne injector,

dx.doi.org/10.1021/np200390x | J. Nat. Prod. 2011, 74, 2505−2513

and a G-1365B multiple wave detector using a Waters XTerra Prep MSC_{18} column (300 × 7.8 mm i.d.).

Plant Material. *Humulus lupulus* cones were purchased from BioPlanta s.a.s., Irsina (MT), Italy (lot no. LTH 1002). A voucher specimen (no. 152) is deposited at the Department of Pharmaceutical and Biomedical Sciences.

Extraction and Isolation. The plant material (250 g) was extracted with EtOH (3 × 1.5 L) for 20 days. The solvent was removed under reduced pressure to afford 36 g of crude extract. Part of the extract (2.5 g) was fractionated on Sephadex LH-20 (100 × 5 cm) using MeOH as the mobile phase. Fifty fractions (8 mL) were obtained. Fractions 24−26 (52.4 mg) were chromatographed by semipreparative HPLC/UV (injections 4 mg/100 μL, flow rate 2.00 mL/min), using H_2O/0.1% TFA as eluent A and CH_3CN/0.1% TFA as eluent B of the mobile phase, to afford humulone (**2**, 7 mg, t_R 16.8 min, at 97% purity). The elution program started with a linear gradient of 20% of eluent B to 100% of B in 60 min. The detection wavelength was 254 nm. Fractions 32−38 (102.6 mg) were chromatographed by semipreparative HPLC/UV (injections 4 mg/100 μL) using H_2O/0.1% TFA as eluent A and CH_3CN/0.1% TFA as eluent B of the mobile phase to afford xanthohumol (**1**, 18 mg, t_R 29.8 min, at 98% purity). The elution program started with a linear gradient of 20% of eluent B to 100% of B in 40 min. The detection wavelength was again 254 nm. Compounds **1** and **2** were identified by comparison of their NMR and MS data with those reported in the literature.[30,31]

Cell Cultures. Human glioblastoma T98G (WHO grade IV) and U87-MG (WHO grade III) cell lines, obtained from ATCC, were cultured in DMEM medium supplemented with 2 mM L-glutamine, 10% heat-inactivated fetal bovine serum, 1% sodium pyruvate, 1% nonessential amino acids, and 1% penicillin/streptomycin (all from Lonza, Switzerland) at 37 °C in a 5% CO_2 humidified incubator. Normal human astrocytes were cultured with an optimized medium for their growth contained in the cell kit (Clonetic Astrocytes Cell System, Lonza). The cells were used up to a maximum of 10 passages.

Reagents and Inhibitors. The general caspase inhibitor Z-VAD-FMK was purchased from BD Pharmingen (BD Bioscience, Bedford, MA, USA), and the p42/44 MAPK (ERK1/2) inhibitor PD98059, the p-38 MAPK inhibitor SB203580, and the JNK inhibitor SP600125 were obtained from Calbiochem (San Diego, CA, USA). 2,7-Dichlorofluorescein diacetate (DCFH-DA) was purchased from Molecular Probes (Eugene, OR), and phorbol myristate acetate, ascorbic acid, *N*-acetyl-L-cysteine, and MTT were obtained from Sigma (Sigma-Aldrich, Italy).

Cell Viability Assay. NHA, T98G, and U87-MG cells (3×10^4) were plated in 96-well culture plates in 90 μL of culture medium and incubated at 37 °C in humidified 5% CO_2. The day afterward, 10 μL aliquots of serial dilutions of xanthohumol (**1**) and humulone (**2**) (1−50 μM) were added, and the cells incubated for 48 h. Cell viability was assessed through the MTT assay.[32] Briefly, 25 μL of MTT (5 mg/mL) was added, and the cells were incubated for an additional 3 h. Thereafter, cells were lysed and the dark blue crystals solubilized with 100 μL of a solution containing 50% *N*,*N*-dimethylformamide and 20% SDS with an adjusted pH of 4.5. The optical density (OD) of each well was measured with a microplate spectrophotometer (Titertek Multiskan MCC/340) equipped with a 620 nm filter. Cell viability in response to treatment was calculated as the percentage of control cells treated with solvent DMSO at the final concentration (0.1%): % viable cells = (100 × OD treated cells)/OD control cells.

Cell Cycle Analysis. Cells were plated at 2×10^5 in a 60 mm dish and exposed to different concentrations of xanthohumol (**1**) and humulone (**2**) (1−40 μM). After the incubation period, cells were harvested and fixed in cold 70% ethanol at −20 °C. Cell cycle profiles were evaluated by DNA staining with 2.5 mg/mL propidium iodide in phosphate-buffered saline supplemented with 100 U/mL ribonucleases A, for 30 min at room temperature. Samples were analyzed with a FACScalibur flow cytometer (Becton Dickinson, CA, USA) using the Cell Quest evaluation program. The distribution of cells in distinct cell cycle phases was determined using ModFit LT cell cycle analysis software.

Analysis of Apoptosis. Apoptosis was analyzed by propidium iodide incorporation into permeabilized cells, and hypodiploid DNA was measured by flow cytometry as described.[33] Briefly, cells were washed in phosphate-buffered saline and resuspended in 500 μL of a solution containing 0.1% sodium citrate, 0.1% Triton X-100, and 50 μg/mL propidium iodide (Sigma-Aldrich, Italy). After incubation at 4 °C for 30 min in the dark, cell nuclei were analyzed with a Becton Dickinson FACScalibur flow cytometer using the Cell Quest program. Cellular debris were excluded from analysis by raising the forward scatter threshold, and the DNA content of the apoptotic nuclei was registered on a logarithmic scale. The percentage of the cells in the hypodiploid region was calculated.

Determination of Intracellular ROS Production. The effect of xanthohumol on ROS was evaluated by measuring dichlorofluorescein fluorescence.[34] T98G cells were incubated for different times (0.5−24 h) in the presence and absence of **1** (20 μM) with or without NAC (5 mM) pretreatment. At the end of the incubation, cells were washed and resuspended (2×10^5 cells/mL) in Hank's balanced salt solution containing 10 μM 2′,7′-dichlorodihydrofluorescein diacetate. Following a further 20 min incubation at 37 °C, DCF fluorescence was monitored by flow cytometry using the Cell Quest program (FL1-H channel). Fluorescence intensity of dichlorofluorescein was observed under a 200 M Zeiss Axiovert fluorescence microscope. Images were acquired using the Axio-vision software package.

Analysis of Mitochondrial Transmembrane Potential (ΔΨm). Mitochondrial membrane potential (ΔΨm) was assessed using flow cytometric analysis of cells stained with tetramethylrhodamine ethyl ester (Sigma Aldrich), as previously described.[35] Cells were incubated with 5 nM tetramethylrhodamine ethyl ester for 30 min at 37 °C, and then fluorescence intensity of tetramethylrhodamine ethyl ester was evaluated by flow cytometry (FL-2 channel).

Total, Cytosolic, and Mitochondrial Protein Extraction. Total intracellular proteins were extracted from the cells by membrane disruption in lysis buffer, 50 mM Tris-HCl, 1% sodium-deoxycholate, 1% SDS, and 0.5% IGEPAL (all from Sigma-Aldrich, Gallarate, Italy), containing protease and phosphatase inhibitors (1 mM PMSF, 1 μg/mL leupeptin, 1 μg/mL pepstatin, 1 μg/mL aprotinin, 1 μM Na_3VO_4, 1 μM NaF; all from Sigma-Aldrich). To obtain cytosolic and mitochondrial fractions, cells were treated with a digitonin buffer (20 mM Hepes-KOH, pH 7.3, 110 mM KAc, 5 mM NaAc, 2 mM MgAc2, 1 mM EGTA, and 200 μg/mL digitonin) on ice for 10 min to permeabilize the cell membrane. The cell lysate was then centrifuged at 10000*g* at 4 °C for 15 min. The supernatant was collected as a cytosolic fraction, and the pellet (mitochondria-containing fraction) was resuspended in 1X-SDS-loading buffer. Protein content was estimated according to a commercial protein assay (Bio Rad, Milan, Italy), and the samples were either analyzed immediately or stored at −80 °C. Total, cytosolic, and mitochondrial extracts were then analyzed by Western blotting.

Western Blotting Analysis. Total, cytosolic (30 μg protein), and mitochondrial samples were loaded into 10−12% acrylamide gels and separated by SDS-PAGE in denaturating conditions at 50 V. The separated proteins were then transferred electrophoretically (100 mA per blot 90 min; Trans Blot Semi-Dry, Bio Rad) to nitrocellulose paper (Immobilon-NC, Millipore, Bedford, MA, USA) soaked in transfer buffer (25 mM Tris, 192 mM glycine, Sigma-Aldrich) and 20% methanol v/v (Carlo Erba, Milan, Italy). Nonspecific binding was blocked by incubation of the blots in 5% nonfat dry-milk powder (Bio Rad) in TBS/0.1% Tween (25 mM Tris; 150 mM NaCl; 0.1% Tween, Sigma-Aldrich) for 60 min. After washing, the blots were incubated overnight at 4 °C with the following primary antibodies: mouse monoclonal anti-PARP (diluted 1:1000), mouse monoclonal anti-Bcl-2 (diluted 1:500), mouse monoclonal anti-cytocrome *c*, rabbit polyclonal anti-caspase-3 (all from Santa-Cruz Biotechnology, DBA Italia s.r.l, Milan, Italy), mouse monoclonal anti-caspase-9 (BioLegend, San Diego, CA, USA), rabbit polyclonal anti-p53 and anti-phospho-p53, rabbit polyclonal anti-p-ERK and ERK1/2 (diluted 1:1000), rabbit polyclonal anti-p-p38 and p38, p-JNK, and JNK (from Cell Signaling Technology, Beverly, MA, USA), and mouse monoclonal anti-β-actin (Sigma-Aldrich, Italy). After incubation with the primary

antibodies and washing in TBS/0.1% Tween, the appropriate secondary antibody, either anti-mouse (diluted 1:5000) or anti-rabbit (diluted 1:5000) (both from Sigma-Aldrich, Italy), was added for 1 h at room temperature. Immunoreactive protein bands were detected by chemiluminescence using enhanced chemiluminescence reagents and exposed to Hyperfilm (both from Amersham Biosciences, Italy). The blots were then scanned and analyzed (Gel-Doc 2000, Bio Rad).

Statistical Analysis. All results are shown as means ± SEM of three experiments performed in triplicate. The optical density of the protein bands detected by Western blotting was normalized on β-actin levels. Statistical comparisons between groups were made using ANOVA followed by the Bonferroni parametric test. Differences were considered significant if $p < 0.05$.

■ ASSOCIATED CONTENT

Ⓢ Supporting Information

Figures S1 and S2 are available free of charge via the Internet at http://pubs.acs.org.

■ AUTHOR INFORMATION

Corresponding Author

*Tel: +39089969744. Fax: ++39089969602. E-mail: annacap@unisa.it (A.C.). Tel: ++39089969763. Fax: ++39089969602. E-mail: piacente@unisa.it (S.P.).

■ ACKNOWLEDGMENTS

The authors gratefully acknowledge the contribution of Prof. L. Parente, University of Salerno, for critically reading the manuscript. The first author is very grateful to young researcher travel grant of the Italian Society of Pharmacology (SIF) to support her visit and research in the laboratory of A.G.R. at CIR at University of Edinburgh.

■ REFERENCES

(1) Sathornsumetee, S.; Rich, J. N. *Ann. N. Y. Acad. Sci.* **2008**, *1142*, 108−132.
(2) Youdim, K. A.; Shukitt-Hale, B.; Joseph, J. A. *Free Radical Biol. Med.* **2004**, *37*, 1683−1693.
(3) Gerhauser, C. *Eur. J. Cancer* **2005**, *41*, 1941−1954.
(4) Zanoli, P.; Zavatti, M. *J. Ethnopharmacol.* **2008**, *116*, 383−396.
(5) Lust, S.; Vanhoecke, B.; Janssens, A.; Philippe, J.; Bracke, M.; Offner, F. *Mol. Nutr. Food Res.* **2005**, *49*, 844−850.
(6) Vanhoecke, B.; Derycke, L.; Van Marck, V.; Depypere, H.; DE Keukeleire, D.; Bracke, M. *Int. J. Cancer* **2005**, *117*, 889−895.
(7) Tobe, H.; Kubota, M.; Yamaguchi, M.; Kocha, T.; Aoyagi, T. *Biosci. Biotechnal. Biochem.* **1999**, *61*, 158−159.
(8) Albini, A.; Dell'Eva, R.; Venè, R.; Ferrari, N.; Buhler, D. R.; Noonan, D. M.; Fassina, G. *FASEB J.* **2006**, *20*, 527−529.
(9) Noonan, D. M.; Benelli, R.; Albini, A. *Recent Results Cancer Res.* **2007**, *174*, 219−224.
(10) Chichirau, A.; Flueraru, M.; Chepelev, L. L.; Wright, J. S.; Willmore, W. G.; Durst, T.; Hussain, H. H.; Charron, M. *Free Radical Biol. Med.* **2005**, *38*, 344−355.
(11) Vogel, S.; Heilmann, J. *J. Nat. Prod.* **2008**, *71*, 1237−1241.
(12) Strathmann, J.; Klimo, K.; Sauer, S. W.; Okun, J. G.; Prehn, J. H.; Gerhäuser, C. *FASEB J.* **2010**, *24*, 2938−2950.
(13) Nordberg, J.; Arnér, E. S. *Free Radical Biol. Med.* **2001**, *31*, 1287−1312.
(14) Meunier, S.; Hanédanian, M.; Desage-El Murr, M.; Nowaczyk, S.; Le Gall, T.; Pin, S.; Renault, J. P.; Boquet, D.; Créminon, C.; Mioskowski, C.; Taran, F. *Chem. Biochem.* **2005**, *6*, 1234−1241.
(15) Ramos, S. *Mol. Nutr. Food Res.* **2008**, *52*, 507−526.
(16) Das, A.; Banik, N. L.; Ray, S. K. *Cancer* **2010**, *116*, 164−176.
(17) Lee, I. S.; Lim, J.; Gal, J.; Kang, J. C.; Kim, H. J.; Kang, B. Y.; Choi, H. J. *Neurochem. Int.* **2010**, *58*, 153−160.
(18) Kluck, R. M.; Bossy-Wetzel, E.; Green, D. R.; Newmeyer, D. D. *Science* **1997**, *275*, 1132−1136.
(19) Monteghirfo, S.; Tosetti, F.; Ambrosini, C.; Stigliani, S.; Pozzi, S.; Frassoni, F.; Fassina, G.; Soverini, S.; Albini, A.; Ferrari, N. *Mol. Cancer Ther.* **2008**, *7*, 2692−2702.
(20) Das, A.; Banik, N. L.; Ray, S. K. *Cancer* **2010**, *116*, 164−176.
(21) Lee, I. S.; Lim, J.; Gal, J.; Kang, J. C.; Kim, H. J.; Kang, B. Y.; Choi, H. J. *Neurochem. Int.* **2010**, *58*, 153−160.
(22) Zhuang, S.; Schnellmann, R. G. *J. Pharmacol. Exp.* **2006**, *319*, 991−997.
(23) Hodnick, W. F.; Ahamad, S.; Pardini, R. S. *Adv. Exp. Med. Biol.* **1998**, *439*, 131−150.
(24) Kong, A. N.; Owuor, E.; Yu, R.; Hebbar, V.; Chen, C.; Hu, R.; Mandlekar, S. *Drug Metab. Rev.* **2001**, *33*, 255−271.
(25) Torres, M.; Forman, H. J. *Biofactors* **2003**, *17*, 287−296.
(26) Arany, I.; Megyesi, J. K.; Kaneto, H.; Price, P. M.; Safirstein, R. L. *Am. J. Physiol., Renal Physiol.* **2004**, *287*, F543−F549.
(27) Kim, Y. K.; Kim, H. J.; Kwon, C. H.; Kim, J. H.; Woo, J. S.; Jung, J. S.; Kim, J. M. *J. Appl. Toxicol.* **2005**, *25*, 374−382.
(28) Dong, J.; Ramachandiran, S.; Tikoo, K.; Jia, Z; Lau, S. S.; Monks, T. J. *Am. J. Physiol., Renal Physiol.* **2004**, *287*, F1049−F1058.
(29) Oda, K.; Arakawa, H.; Tanaka, T.; Matsuda, K.; Tanikawa, C.; Mori, T.; Nishimori, H.; Tamai, K.; Tokino, T.; Nakamura, Y.; Taya, Y. *Cell* **2000**, *102*, 849−862.
(30) Tabata, N.; Ito, M.; Tomoda, H.; Omura, S. *Phytochemistry* **1997**, *46*, 683−687.
(31) Hoek, A. C.; Hermans-Lokkerbol, A. C. J.; Verpoorte, R. *Phytochem. Anal.* **2001**, *12*, 53−57.
(32) Mosmann, T. *J. Immunol. Methods* **1983**, *65*, 55−63.
(33) Riccardi, C.; Nicoletti, I. *Nat. Protoc.* **2006**, *1*, 1458−1461.
(34) Rothe, G.; Valet, G. *J. Leukocyte Biol.* **1990**, *47*, 440−448.
(35) Scaduto, R. C. Jr.; Grotyohann, L. W. *Biophys. J.* **1999**, *76*, 469−477.